Desalination and Water Treatment
www.deswater.com

doi: 10.5004/dwt.2017.0958

58 (2017) 249–257
January

Adsorption of chloride ions from aqueous solution on γ-alumina modified by sodium oxide: an equilibrium and kinetics study

Masoud Gerami[a], Rouein Halladj[b,*], Rouholamin Biriaei[b], Sima Askari[c], Mehdi Nazari[a]

[a]*Department of Petrochemical Engineering, Amirkabir University of Technology, Mahshahr Campus, P.O. Box 415, Mahshahr, Iran, Email: gerami1776@yahoo.com (M. Gerami), msnazari@aut.ac.ir (M. Nazari)*
[b]*Department of Chemical Engineering, Amirkabir University of Technology, P.O. Box 15875-4413, Hafez Ave, Tehran, Iran, Tel. 00982164543151; Fax: +98 21 66405847; email: halladj@aut.ac.ir (R. Halladj), biryaee.rouholamin@aut.ac.ir (R. Biriaei)*
[c]*Department of Chemical Engineering, Science and Research Branch, Islamic Azad University, Tehran, Iran, Email: sima.askari@aut.ac.ir*

Received 10 August 2013; Accepted 13 June 2016

ABSTRACT

Fine particles of the gamma-alumina adsorbent were chemically prepared by impregnating with an aqueous solution of sodium nitrate as precursor to get a novel Na-doped composite material with enhanced dechloridation capacity. The resultant sodium oxide coated alumina was characterized using Fourier transform infrared, X-ray diffraction, high-resolution scanning electron microscopy and Brunauer–Emmett–Teller analyses. The chloride uptake efficiency of the prepared sodium oxide coated alumina was examined and compared with the unmodified conventional γ-Al_2O_3 upon batch adsorption experiments. Solution pH (3–10), initial chloride concentration (20–100 mg/L) and contact time (30–180 min), as the most important factors in the adsorption process, were also investigated at temperature of 35°C. The modified γ-Al_2O_3 adsorbent showed a high sorption capacity equal to11.25 mg/g at C_0 = 100 ppm, pH = 6, contact time = 180 min, temperature = 35°C and adsorbent dosage of 8 g/L. The experimental adsorption equilibrium and kinetic data closely followed the Langmuir adsorption isotherm and pseudo-second-order kinetic model, respectively. The sodium impregnated γ-Al_2O_3 showed better chloride removal properties due to the incorporation of electropositive sodium oxide particles which enhanced both selectivity and adsorptive properties of the sorbent.

Keywords: Dechloridation; Sodium oxide coated alumina; Kinetics; Isotherms

1. Introduction

In general, chloride in drinking water originates from natural sources, sewage and industrial effluents, urban run-off containing deicing salt, leachate from landfills, irrigation drainages and saline intrusion [1,2]. In addition, chloride is a deleterious ionic species in cooling water systems because it promotes corrosion, and limits the cycles of concentration, and most of the inhibitors are sensitive to chloride concentration in the water [2–4]. The threshold concentration of chloride above which pitting of iron is possible is reported to be about 10 mg/L [1]. The technologies that are under most active consideration for removing excessive free chloride (Cl^-) contents are: reverse osmosis, ion exchange, electrodialysis and adsorption. With the exception of the adsorption process because of its simplicity and the availability of a wide range of adsorbents, these technologies are very expensive and have many operating problems [5,6]. The adsorption process seems to be the most versatile and effective treatment method if combined with appropriate regeneration steps, especially for small community water sources [7,8].

* Corresponding author.

Alumina-based materials have received considerable attention as potential adsorbents for wastewater treatment. Their uptake of contaminants from aqueous solutions has been studied; these include reactive arsenate, arsenide, fluoride, bromate, phosphate, bromide, selenite, borate, nitrate and chromate [9–14].

The advantages of γ-Al_2O_3 as a sorbent lie in the fact that it possesses high surface area, mechanical strength and positively charged surface functional groups which produce strong affinity for negatively charged ions [7,15]. It is also known that the activity of alumina depends on its chemical properties as well as structural phases [16].

To the best of our knowledge, the application of γ-alumina and sodium oxide coated alumna in dechloridation has not been reported yet. Thus, it is worthwhile to assess the performance of sodium oxide coated alumina as a novel adsorbent in chloride removal compared with unmodified γ-Al_2O_3. Moreover, the effects of solution pH, contact time, adsorbent dosage and initial Cl^- concentration on the uptake efficiency of the synthesized adsorbent have been studied through batch tests. The Langmuir, Freundlich and Dubinin–Kaganer–Radushkevich (DKR) isotherms were used to correlate adsorption equilibrium data and to get an insight into the chloride adsorption mechanism. The pseudo-first-order, pseudo-second-order and intraparticle diffusion kinetic models were also applied in order to study the dynamic aspects of the adsorption process. The mechanism of binding chloride anions by the composite adsorbent was also elucidated.

2. Experimental

2.1. Materials

All chemicals used in the present study were of analytical reagent grade. Millipore deionized water was used in all the experiments. A stock solution of 1,000 mg/L chloride was prepared by dissolving appropriate amounts of sodium chloride (Sigma-Aldrich, St. Louis, Missouri, United States) in double-distilled water. The entire standard and chloride spiked solutions for removal experiments and analyses were prepared by appropriate dilution from the freshly prepared stock solution. The γ-Al_2O_3 used in this study was obtained through dehydration and heat treatment of a well crystallized synthetic boehmite (γ-AlOOH) precursor (CERA hydrate, purchased from a local commercial source).

2.2. Characterization of the sorbent

Fourier Transform Infrared (FTIR) spectra of the samples in the form of KBr pellets were collected using a Nicolet 8700 FTIR spectrometer (Thermo Instruments, USA) in the wavelength range of 4,000–400 cm^{-1}. The Brunauer–Emmett–Teller (BET) surface area, pore volume and average pore radius of the adsorbent were measured by a multipoint N_2 adsorption–desorption isotherm at liquid nitrogen temperature (77 K) using a NOVA 2000 series instrument (Quantachrome, USA). Also, the morphology and size of the particles were studied by high-resolution scanning electron microscope (HR-SEM) images which were obtained using a Quanta 200 (FEI, Netherlands) field emission gun (FEG) operating at 4 kV. Phase structure analysis was carried out by an X-ray diffractometer (XRD; Bruker Model No. D8ADVANCE) using Ni filtered Cu kα ($\lambda_{Cu\ k\alpha}$ = 1.54056 Å, radiation at 40 kV) over the 2θ range of 5–90°. The obtained experimental patterns were compared with the standards compiled by the Joint Committee on Diffraction Pattern and Standards (JCDPS).

2.3. Preparation of impregnated alumina

Powdered γ-Al_2O_3 fine particles were obtained through the calcination of highly crystalline synthetic boehmite. Each boehmite precursor was calcined at temperatures of 700°C–800°C with a heating rate of 5°C/min. In order to prepare sodium oxide coated alumina, 5 g of preformed fine powder of γ-Al_2O_3 and 200 mL aqueous solution of sodium (0.02 M) were mixed together in a 250 mL round-bottom glass flask. The resultant suspension was finely stirred at temperature of 80°C for 5 h using a Heidolph rotary evaporator with continuous rotating at 150 rpm. Before evacuating the chamber, ammonia solution (24 wt.%) was added dropwise to the as-made mixture under vigorous stirring in order to yield a transparent gel. After aging the supernatant liquid for 12 h at 100°C, the aqueous phase was removed completely from the paste under vacuum condition in the evaporator. The impregnated γ-Al_2O_3 was then filtered, rinsed and finally calcined under air atmosphere at 600°C for 4 h. The resultant product was finely milled and sieved, and the fine powder (mesh < 125 μm) of impregnated γ-Al_2O_3 was used for the experiments.

2.4. Sorption experiments

The experimental solutions for adsorption and analysis were prepared freshly by diluting the stock solution. A series of 50 mL Erlenmeyer flasks of chloride ions solutions containing a predetermined dose of the adsorbent were kept in a magnetic shaker with continuous stirring for specified adsorption time intervals in order to reach equilibrium. The pH of the solution was adjusted by using dilute NaOH or HNO_3 solution. After the specified time intervals, the solution was then filtered using a Whatman filter paper No. 42, and the filtrate was analyzed for residual chloride concentration by ultraviolet-visible spectrophotometer (Varian, Australia) at a wavelength of 463 nm. The clear liquid filtrate was also analyzed by inductively coupled plasma–atomic emission spectroscopy (ICP-AES, Model OPTIMA 4100DV) to detect any trace amounts of leached sodium from the synthetic adsorbent.

To evaluate the chloride removal efficiency and the adsorption capacity, initial chloride concentration (20–100 mg/L), effect of solution pH (3–11), contact time (15–270 min) and adsorbent dosage (2–10 g/L) were investigated in batch mode experiments. The pH of experimental solutions was adjusted using 0.01 M HNO_3 and 0.01 M NaOH solutions. In all the experiments, the Cl^- removal percentage and adsorption capacity (mg/g) were calculated using following expressions, respectively:

$$\%\text{Removal} = \frac{C_o - C_e}{C_o} \times 100 \quad (1)$$

$$q_e = (C_o - C_e) \times \frac{v}{m} \quad (2)$$

All the adsorption experiments were carried out three times, and the average values were used for validation (relative deviation less than 3.0%).

3. Results and discussion

3.1. The characteristics of the adsorbents

Figs. 1(a) and 1(b) show the XRD patterns of the γ-Al_2O_3 particles and as-prepared modified γ-Al_2O_3, respectively. In Fig. 1(a) there are diffraction peaks which have mainly appeared in 2θ ≈ 32°, 37.8°, 46° and 67°. After surface modification of bare alumina with sodium oxide, new crystalline phases will mainly appear at 2θ ≈ 28°, 32.6° and 46.3° (Fig. 1(b)) which are identified as Na_2O according to the JCPDS file No. 23-0528. The weak peaks appeared in Fig. 1(b) indicate that the degree of crystallinity of the coated alumina is lower than that of the bare alumina.

The FTIR results of the bare γ-Al_2O_3 and modified γ-Al_2O_3 are depicted in Fig. 2. The characteristic infrared absorption peak of alumina was detected at 740 cm^{-1}. Additionally, two bands also appeared at 1,404 and 582 cm^{-1} in the spectrum, which are the characteristics of Al–O and Al–H stretching vibrations in Al_2O_3 [15]. The peaks at 3,450 and 1,638 cm^{-1} correspond to the stretching and bending vibration modes of OH bonds (on the surface of Al_2O_3), respectively [17].

Upon incorporation of sodium oxide onto the γ-Al_2O_3, no serious structural modifications will occur in γ-Al_2O_3 as illustrated in Fig. 2. However, the decrease in some peak intensities of impregnated alumina as compared with γ-Al_2O_3 indicates the existence of some interactions between surface functional groups of γ-Al_2O_3 and sodium oxide [17].

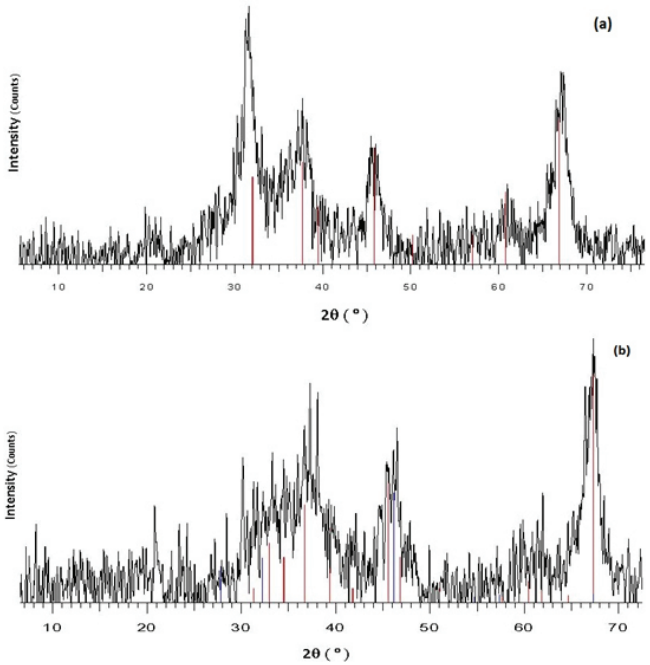

Fig. 1. XRD spectra of (a) the bare γ-Al_2O_3 and (b) the sodium incorporated γ-Al_2O_3.

The SEM image of the bare γ-Al_2O_3, obtained by calcining a boehmite precursor, is shown in Fig. 3(a) which depicts relatively well ordered rocks like surface structure which seems to be a direct consequence of the calcination procedure applied for the boehmite precursor. The estimated elemental composition of γ-Al_2O_3 was 58.13 and 41.87 wt.%, which accounts for Al and O, respectively (Fig. 3(b)). As is evident from Fig. 4(a), a thin layer of Na_2O particles were coated on γ-Al_2O_3 which have almost covered the entire surface of the bare alumina. The estimated wt.% of Al, O and Na elements in the coated alumina (Fig. 4(b)) were also found to be 60.2, 36.95 and 2.77 wt.%, respectively, which are close to the molar ratio of sodium oxide to alumina in the precursor solution.

Table 1 illustrates the BET parameters of the bare alumina. As can be seen from Table 2, the Na_2O impregnated γ-alumina has lower surface area and pore volume than the

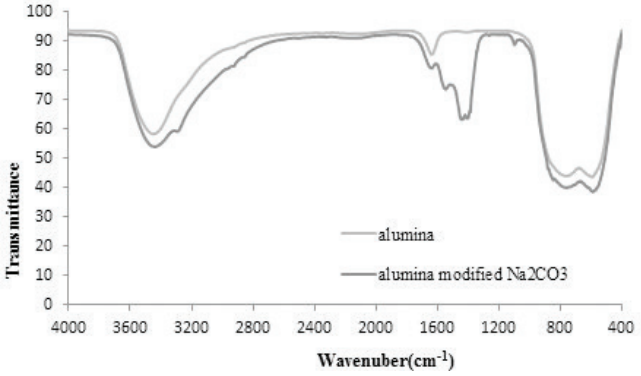

Fig. 2. FTIR spectra of the bare γ-Al_2O_3 and sodium incorporated γ-Al_2O_3.

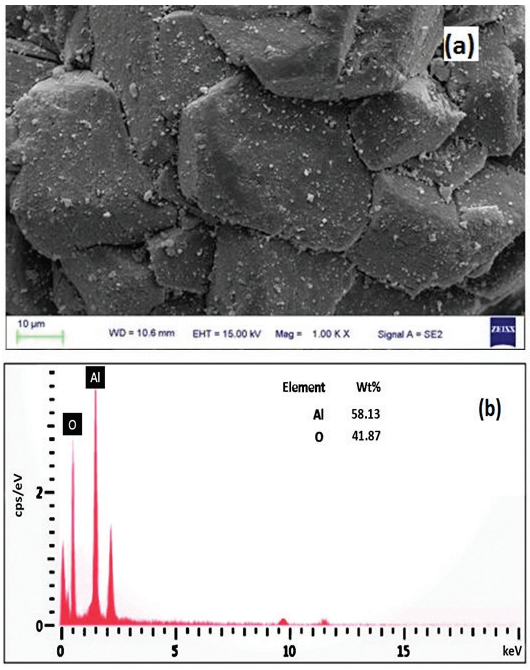

Fig. 3. SEM image of (a) the boehmite derived γ-Al_2O_3 support and (b) EDAX spectra of γ-Al_2O_3 support.

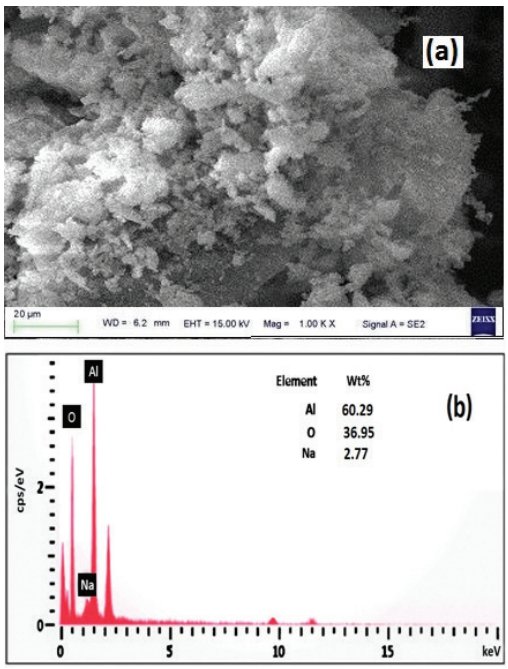

Fig. 4 SEM image of (a) the sodium incorporated γ-Al_2O_3 and (b) EDAX spectra of sodium incorporated γ-Al_2O_3.

Table 1
Characteristics and chemical composition of γ-Al_2O_3

Item	Value
Particle size	>0.2 mm (less than 2.0%) <0.063 mm (less than 28.0%) >0.063 mm (more than 72.0%)
Specific surface area (BET)	190 m^2/g.
Loss on ignition (1,000°C, 2 h)	1.0 wt.%
Pore volume	0.37 (cm^3/g)
Bulk density	950 g/L
Components (wt.%)	Al_2O_3 (99.81) SiO_2 (0.04) Fe_2O_3 (0.04) Na_2O (0.11)

Table 2
BET and Barrett-Joyner-Halenda (BJH) parameters of the sodium incorporated γ-Al_2O_3

Parameter	Value
BET (m^2/g)	90.70
Pore volume (cm^3/g)	0.22
Pore diameter (Å)	46.40

unmodified one which can tentatively be assigned to filling parts of the alumina pores as a result of diffusion of impregnating particles [18]. In addition, the point of zero charge (pH_{PZC}) of the promoted adsorbent was determined through the reported method in [19] and found to be *ca*. 6.5.

3.2. Initial evaluation of the adsorbents performance

The performance of unmodified alumina and impregnated alumina adsorbents in terms of adsorbed Cl^{-1} ion in the test solution were compared under the following conditions: adsorbent dose of 0.4 g/50 ml; C_0 = 20, 40, 60, 80 and 100 mg/L; pH = 6.3 ± 0.3; 150 rpm at 35°. The results of adsorption of Cl^{-1} ions after 270 min on unmodified alumina as the base material are summarized in Table 3. Fig. 5 also shows the kinetics of chloride removal which clearly reveals an improved chloride capacity and faster sorption kinetics onto the sodium oxide coated alumina adsorbent. With the passage of time, the active sites on the adsorbent are gradually covered. Then, the rate of chloride ions uptake becomes slower and finally reaches a plateau corresponding to the adsorption equilibrium. It is clear that the removal of chloride ions increased with an increase in contact time; however, no further significant increase was observed after 180 min. Therefore, the minimum contact time required to reach equilibration was considered to be at least 180 min.

3.3. Effect of pH

According to the literature, pH plays an important role in sorption processes at solution–sorbent interfaces [20–22]. As shown in Fig. 6, the chloride ions uptake by the modified alumina was studied over a pH range of 3–11 with an adsorbent dose of 8 g/L, initial chloride concentration of 100 mg/L, shaking speed of 150 rpm and contact time of 180 min. The initial pH was adjusted using 0.1 N NaOH or 0.1 N HNO_3 solutions. The sorption of chloride on the

Table 3
Adsorption of chloride ions on unmodified alumina

Initial concentration (mg L^{-1})	Final concentration (mg L^{-1})	% Adsorption
20	18	10
40	37	7.5
60	45	25
80	52	35
100	58	42

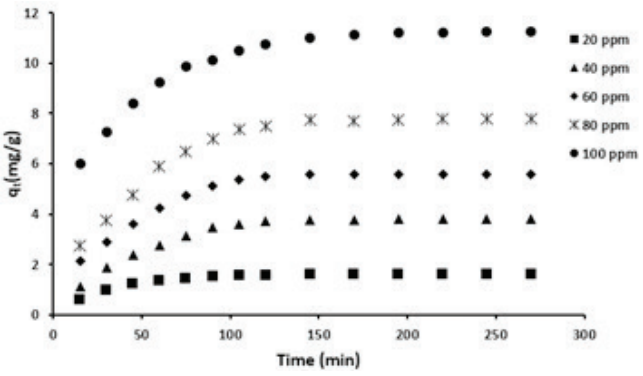

Fig. 5. Chloride depletion rate as a function of contact time on sodium incorporated γ-Al_2O_3 (C_0 = 20–100 mg/L, temperature = 35°C, pH = 6.3 ± 0.3).

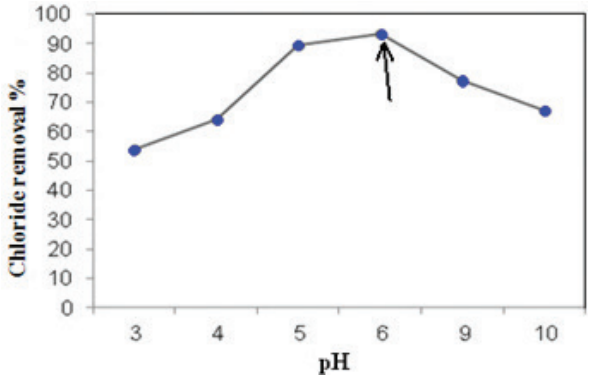

Fig. 6. Effect of pH on chloride adsorption by modified γ-alumina (contact time = 180 min, C_0 = 100 mg/L, adsorbent dose = 8 g/L and shaker speed = 150 rpm).

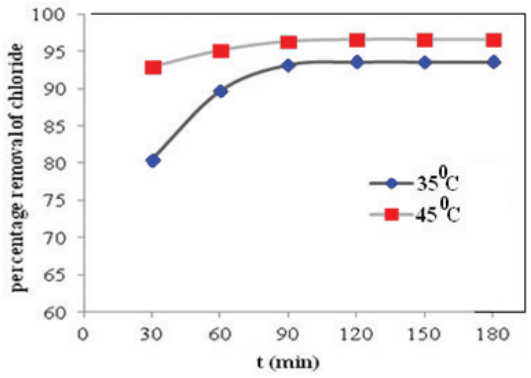

Fig. 7. Effect of temperature on chloride uptake by modified γ-alumina (contact time = 180 min, pH = 6.3 ± 0.3, adsorbent dose = 8 g/L).

modified alumina initially increased with increasing pH, and thereafter reached a maximum of 93.14% at pH = 6.3 ± 0.3 and then decreased with a further increase in pH. It can be concluded that in pHs below the zero point of charge of the adsorbent, the surface is positively charged which consequently attracts the Cl^- ions. The decrease in removal of chloride at alkaline pHs can be attributed to the competition for the active sites by OH^- ions and the electrostatic repulsion of anionic chlorides by the negative surface charge of modified alumina particles [21,22].

3.4. The effect of solution temperature

The adsorption of chloride ions was carried out at two different temperatures, 308 and 318 K, using modified γ-alumina as adsorbent (Fig. 7). The experimental results showed that the removal percentage of chloride increases with an increase in the solution temperature. However, this increment is very slight and can be neglected [23].

3.5. Effect of initial concentration

The adsorption of Cl^- ions onto the Na_2O impregnated γ-Al_2O_3 was studied under the following conditions: adsorbent dose of 8 g/L; C_0 = 20, 40, 60, 80 and 100 mg/L; pH = 6.3 ± 0.3; 150 rpm at 35°. The results presented in Fig. 8 show that with an increase in the initial concentration from 20 to 100 mg/L, the removal rate increased from 64.4% to 93.1%. This may be due to the high initial concentrations resulting in the higher concentration gradient (driving force) which can overcome all possible external mass transfer resistances [22,24].

3.6. Modeling of adsorption kinetics

Dynamic aspects of the adsorption process in terms of the order and the rate constant can be evaluated through analyzing the kinetic adsorption data by the following well-known Eqs. (3)–(5) [25–29]:

- Pseudo-first-order

$$\ln(q_e - q_t) = \ln q_e - k_1 t \quad (3)$$

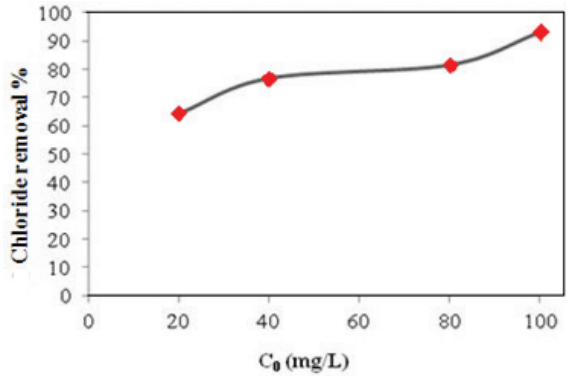

Fig. 8. Effect of initial chloride concentration on chloride removal efficiency of sodium incorporated γ-Al_2O_3 (temperature = 35°C, contact time = 180 min, sorbent dose = 8 g/L).

- Pseudo-second-order

$$\frac{t}{q_t} = \frac{1}{k_2 q_e^2} + \frac{1}{q_e} t \quad (4)$$

- Intra-particle diffusion

$$q_t = k_{diff} . t^{0.5} \quad (5)$$

The agreement between the calculated and experimental value of q_e and correlation coefficient (R^2), were considered as a criterion for judgment on the applicability of pseudo-first-order and pseudo-second-order models. The kinetic parameters of pseudo-first-order and pseudo-second-order models that are given in Tables (4) and (5) were calculated using the linear regression method from Fig. 9. The higher R^2 and lower k_2 values under all concentrations suggest that the depletion rate of chloride might be potentially governed by the pseudo-second-order reaction mechanism. This could also be confirmed considering the calculated q_e and experimental q_e (Fig. 5) values. It is also noteworthy to mention that the kinetic rate constants (from Tables 4 and 5) were deeply influenced by initial Cl^- concentration.

Table 4
Pseudo-first-order kinetic model parameters obtained for different initial Cl^- concentrations on modified adsorbent (temperature = 35°C , dosage = 8 g/L, pH = 6.3 ± 0.3, C_0 = 20–100 mg/L)

Initial Cl^- concentration (mg/L)	q_e (mg/g) experimental	k_1 (1/min)	q_e (mg/g) calculated	R^2
20	1.625	0.033	1.96	0.98
40	3.88	0.035	4.49	0.96
60	5.79	0.041	11.8	0.93
80	7.95	0.035	13.3	0.93
100	11.25	0.027	9.02	0.97

Table 5
Pseudo-second-order kinetic model parameters obtained for different initial Cl– concentrations on modified adsorbent (temperature = 35°C, dosage = 8 g/L, pH = 6.3 ± 0.3, C_0 = 20–100 mg/L)

Initial Cl^- concentration (mg/L)	q_e (mg/g) experimental	k_2 (g/mg.min)	q_e (mg/g) calculated	R^2
20	1.625	0.036	1.7	0.997
40	3.88	0.011	3.98	0.991
60	5.79	0.0077	6.2	0.994
80	7.95	0.0056	8.43	0.993
100	11.25	0.005	11.9	0.999

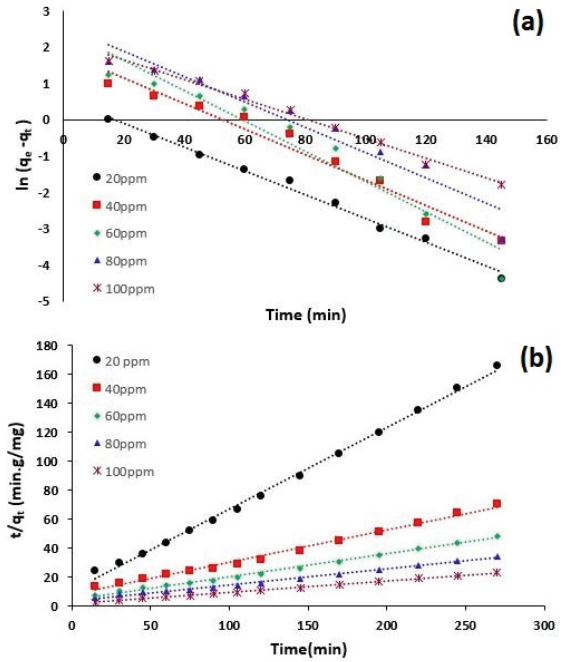

Fig.9. (a) Pseudo-first-order and (b) pseudo-second-order kinetic model plots for chloride sorption onto the coated alumina (pH = 6.3 ± 0.3, dosage = 8 g/L, temperature = 35°C).

In order to investigate the contribution of intraparticle diffusion in the adsorption process, the obtained kinetic data were fitted to Eq. (5). A non-linear regression method (NLRM) was applied to experimental data (Fig. 10) in order to calculate the intraparticle diffusion rate constants which are given in Table 6. The main feature of Fig. 10 is that the linear part of the curves does not pass through the origin indicating a complex nature of the adsorption process on this adsorbent. Indeed, it seems that a combination of surface reaction and diffusion into the adsorbent pores would result in the adsorptive removal of Cl^- ions.

3.7. Adsorption isotherms

In order to evaluate the chloride adsorption capacity of the sodium impregnated γ-Al_2O_3, two frequently used equilibrium models, the Langmuir and Freundlich isotherms, were employed [27,30]:

$$q_e = \frac{(q_m k_1)C_e}{1+(q_m k_L)C_e} \quad (6)$$

$$q_e = k_f . C_e^{1/n} \quad (7)$$

Plotting q_e vs. C_e (Fig. 11) and applying the NLRM give the isotherm parameters given in Table 7.

Table 6
Intraparticle diffusion Weber and Moris model parameters on modified adsorbent (temperature = 35°C, dosage = 8 g/L, pH = 6.3 ± 0.3, C_0 = 20–100 mg/L)

Initial Cl^- concentration (mg/L)	k_{intra} (1/min)	R^2
20	0.1462	0.9525
40	0.1310	0.9835
60	0.1136	0.9905
80	0.0929	0.9935

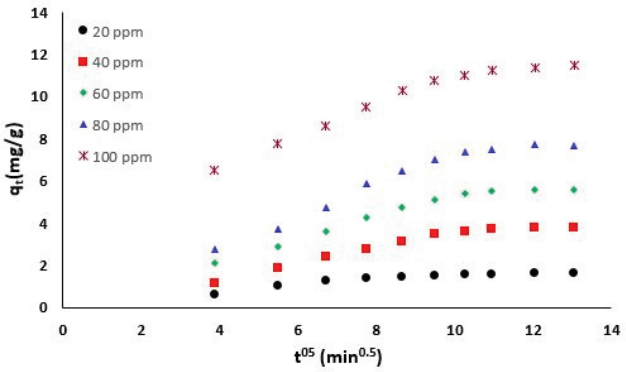

Fig. 10. Intraparticle diffusion model plots for chloride sorption onto the sodium incorporated alumina supported (pH = 6.3 ± 0.3, dosage = 8 g/L, temperature = 35°C

Since the values of the constant 1/n (adsorption intensity) are less than unity, it can be concluded that the adsorption process is favorable during which the adsorption capacity is slightly suppressed at lower equilibrium concentrations [7,22]. As it is evident from the results of Table 7, the chloride ions removal by Na_2O/γ-Al_2O_3 follows the Freundlich isotherm model with a correlation coefficient of 0.99.

Furthermore, the equilibrium data were fitted to the linear form of the DKR adsorption model as well [31]:

$$\ln q_{ed} = \ln q_{md} - K\varepsilon^2 \quad (8)$$

This model has been widely used to explain energetic heterogeneity of the solid surface at the monolayer region in micro-pores [22,32]. The Polanyi potential (ε) can be obtained from Eq. (9):

$$\varepsilon = RT\left(\ln\left(1+\frac{1}{C_e}\right)\right) \quad (9)$$

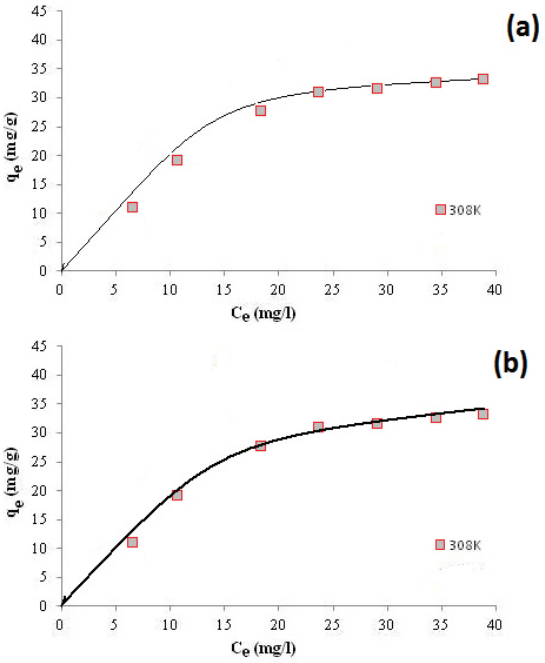

Fig. 11. Modeling of equilibrium adsorption data of chloride uptake on modified γ-Al_2O_3 through (a) Langmuir and (b) Freundlich isotherm model (contact time = 180 min, adsorbent dose = 8 g/L, pH = 6.3 ± 0.3).

The values of adsorption energy, E (kJ/mole), can be expressed as [33]:

$$E = \frac{1}{(-2K)^{0.5}} \quad (10)$$

A plot of $\ln q_{ed}$ vs. ε^2 is shown in Fig. 12. The values of q_{md}, K and thus the adsorption energy (E (kJ/mol)) were obtained from the intercept and slope of the fitted line. The fitting results were presented in Table 8 which shows that the value of free energy is less than 8.0 kJ/mole. It implies that the type of adsorption is physical due to weak Van der Waals forces [26,34].

3.8. Dechloridation mechanism on composite adsorbent

As reported in the literature, anion adsorption involves a chemical interaction between the adsorbent surface and the ions followed by binding them to the sites which mainly reside on the adsorbent surface by means of ion exchange. In the case of sodium oxide coated alumina, incorporation of electropositive metal oxides, that is, sodium oxide, enhances

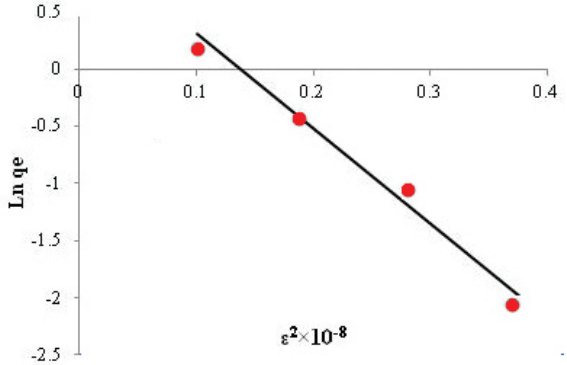

Fig. 12. DKR isotherms obtained using linear method for the adsorption of chloride on modified γ-alumina (pH = 6.3 ± 0.3, C_0 = 100 mg/l, temperature = 35°C).

Table 8
The DKR constants for the adsorption of chloride on sodium incorporated γ-Al_2O_3 at 35°C

Temperature (°C)	DKR constants			
	q_{md} (mmol/g)	K (mol²/kJ²)	E (kJ/mol⁻¹)	R^2
35	2.031	8.299	0.25	0.912

Table 7
The Langmuir and Freundlich isotherm constants for chloride removal by modified adsorbent (dosage = 8 g/L, pH = 6.3 ± 0.3, C_0 = 20–100 mg/L)

Langmuir isotherm model parameters				Freundlich isotherm model parameters		
q_{max} (mg/g)	$k_{Langm.}$ (L/mg)	R_L	R^2	1/n	$k_{Freundlich}$ (mg/g) (L/mg)$^{1/n}$	R^2
11.25	0.876	0.60	0.87	0.95	1.13	0.994

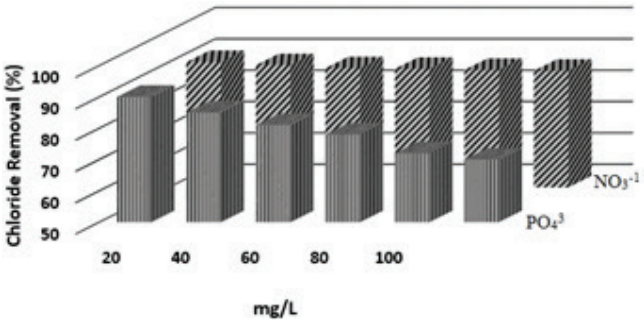

Fig. 13. Effect of some interfering ions on the chloride uptake of the composite adsorbent. (pH = 6.3 ± 0.3, C_0 = 100 mg/l, temperature = 35°C).

the selectivity and adsorptive properties of the resulting composite adsorbent towards negatively charged chloride ions through the following ion exchange mechanism:

$$NaOH + H^+ + Cl^- \leftrightarrow NaCl + H_2O \quad (11)$$

The proposed mechanism coincides well with the adsorption data obtained here which reveals a gradual increase in the pH of solutions as a result of replacement of OH^- with Cl^- during the adsorption process.

3.9. Effect of competing anions on chloride adsorption

The effect of presence of other ions such as PO_4^{3-} and NO_3^{-1} on the chloride removal is presented in Fig. 13. The chloride concentration was considered 100 mg/L while the initial concentration of $HCO3^{-1}$ and NO_2^{-1} ions varied from 0 to 100 mg/L. Some ions may enhance repulsion forces, and some may also compete with for the active sites. The results show that the chloride adsorption is slightly affected in the presence of $NO3_3^{-1}$. On the other hand, a significant effect on the removal efficiency of chloride ions can be seen when PO_4^{3-} ions are available in the solution.

4. Conclusions

The sodium oxide incorporated γ-Al_2O_3 adsorbent was prepared by the wet impregnation method and followed by precipitation and calcinations and then characterized using the BET, SEM, XRD and FTIR techniques. The results showed that the modified alumina adsorbent holds a great potential to be more effective for chloride removal from water sources compared with the unmodified one.

The following conclusions can be drawn from this investigation according to dechloridation properties of the composite adsorbent:

- At the same operating conditions, the modified alumina adsorbed more chloride ions from aqueous solutions compared with the unmodified one.
- The adsorbent dosage, solution pH, initial chloride concentration and contact time were found to be the most important factors in the adsorption process. The maximum sorption capacity of this composite adsorbent was 11.25 mg/gat C_0 = 100 ppm, pH = 6, contact time = 180 min, temperature = 35°C and adsorbent dosage of 8 g/L.
- The experimental adsorption equilibrium and kinetic data closely followed the Langmuir adsorption isotherm and pseudo-second-order kinetic model, respectively. The predicted adsorption energy showed a physical adsorption through Van der Walls forces. The experimental data revealed that the chloride adsorption on the modified alumina is complex and a combination of surface adsorption and diffusion within the pores of the modified alumina contribute to the adsorptive removal of chloride ions.

Nomenclature

C_0	_	Initial concentration of chloride, mg/L
C_e	_	Equilibrium concentration of chloride in the solution, mg/L
V	_	Sorbent free solution volume, L
m	_	Sorbent mass, g
q_e	_	Amount of chloride ions adsorbed at equilibrium, mg/g
q_{max}	_	Maximum sorption capacity (mg/g) upon the Langmuir isotherm model, mg/g
k_L	_	The Langmuir adsorption constant, L/mg
R_L	_	Separation factor or equilibrium parameter
k_F	_	The Freundlich constant which indicates relative adsorption capacity of the sorbent, (mg/g).(mg/L)^n
n	_	The Freundlich constant which indicates adsorption intensity
q_{ed}	_	Amount of chloride adsorbed per unit weight of adsorbent upon DKR adsorption isotherm, mmol/g
q_{md}	_	The DKR isotherm monolayer adsorption capacity, mmol/g
K	_	The DKR isotherm constant related to energy, mol^2/kJ^2
ε	_	The Polanyi potential, kJ^2/mol^2
E	_	Mean sorption energy, kJ/mol
R	_	Universal gas constant, J/mol.K
T	_	Absolute temperature, K
k_1	_	Pseudo-first-order rate constant of adsorption, min^{-1}
k_2	_	Pseudo-second-order rate constant of adsorption, min^{-1}
q_t	_	Amount of chloride uptake at any time, mg/g
$K_{diff.}$	_	The intraparticle diffusion rate constant, mg/g/min$^{1/2}$

References

[1] WD-DWGB-3-17 Sodium and chloride in drinking water. In: *New Hampshire Department of Environmental Services* (2010).
[2] T. Kameda, Y. Miyano, T. Yoshioka, M. Uchida, A. Okuwaki, New treatment methods for waste water containing chloride ion using magnesium-aluminum oxide, Chem. Lett., 29 (2000) 1136–1137.
[3] L. Lv, J. He, M. Wei, D.G. Evans, X. Duan, Uptake of chloride ion from aqueous solution by calcined layered double hydroxides: equilibrium and kinetic studies, Water Res., 40 (2006) 735–743.
[4] R. Hamidi, P. Kazemi, Kinetics and mechanism of sorption of chloride ion from sodium carbonate manufacturing wastewater by Mg–Al oxide, Desalin. Water Treat., 54 (2015) 332–341.

[5] M. Masson, G. Deans, Membrane filtration and reverse osmosis purification of sewage: secondary effluent for re-use at Eraring Power Station, Desalination, 106 (1996) 11–15.
[6] K. Vaaramaa, J. Lehto, Removal of metals and anions from drinking water by ion exchange, Desalination, 155 (2003) 157–170.
[7] T.K. Naiya, A.K. Bhattacharya, S.K. Das, Adsorption of Cd(II) and Pb(II) from aqueous solutions on activated alumina, J. Colloid Interface Sci., 333 (2009) 14–26.
[8] K.M. Parida, A.C. Pradhan, J. Das, N. Sahu, Synthesis and characterization of nano-sized porous gamma-alumina by control precipitation method, Mater. Chem. Phys., 113 (2009) 244–248.
[9] T.-T. Zheng, Z.-X. Sun, X.-F. Yang, A. Holmgren, Sorption of phosphate onto mesoporous gamma-alumina studied with in-situ ATR-FTIR spectroscopy, Chem. Cent. J., 6 (2012) 26.
[10] Y.-S.R. Chen, J.N. Butler, W. Stumm, Adsorption of phosphate on alumina and kaolinite from dilute aqueous solutions, J. Colloid Interface Sci., 43 (1973) 421–436.
[11] Y.S.R. Chen, J.N. Butler, W. Stumm, Kinetic study of phosphate reaction with aluminum oxide and kaolinite, Environ. Sci. Technol., 7 (1973) 327–332.
[12] N. Chubar, New inorganic (an)ion exchangers based on Mg–Al hydrous oxides: (alkoxide-free) sol–gel synthesis and characterisation, J. Colloid Interface Sci., 357 (2011) 198–209.
[13] A. Halajnia, S. Oustan, N. Najafi, A.R. Khataee, A. Lakzian, The adsorption characteristics of nitrate on Mg–Fe and Mg–Al layered double hydroxides in a simulated soil solution, Appl. Clay Sci., 70 (2012) 28–36.
[14] X.-Y. Yu, T. Luo, Y. Jia, R.-X. Xu, C. Gao, Y.-X. Zhang, J.-H. Liu, X.-J. Huang, Three-dimensional hierarchical flower-like Mg-Al-layered double hydroxides: highly efficient adsorbents for As(v) and Cr(vi) removal, Nanoscale, 4 (2012) 3466–3474.
[15] Y. Tang, X. Guan, T. Su, N. Gao, J. Wang, Fluoride adsorption onto activated alumina: modeling the effects of pH and some competing ions, Colloids Surf., A, 337 (2009) 33–38.
[16] S.P. Kamble, G. Deshpande, P.P. Barve, S. Rayalu, N.K. Labhsetwar, A. Malyshew, B.D. Kulkarni, Adsorption of fluoride from aqueous solution by alumina of alkoxide nature: batch and continuous operation, Desalination, 264 (2010) 15–23.
[17] M. Nazari and R. Halladj, Adsorptive removal of fluoride ions from aqueous solution by using sonochemically synthesized nanomagnesia/alumina adsorbents: an experimental and modeling study, J. Taiwan Inst. Chem. Eng., 45 (2014) 2518–2525.
[18] G.R. Moradi, M. Nazari, F. Yaripour, Statistical analysis of the performance of a bi-functional catalyst under operating conditions of LPDME process, Chem. Eng. J., 140 (2008) 255–263.
[19] Y.F. Jia, B. Xiao, K.M. Thomas, Adsorption of metal ions on nitrogen surface functional groups in activated carbons, Langmuir, 18 (2002) 470–478.
[20] S.S. Tripathy, J.-L. Bersillon, K. Gopal, Removal of fluoride from drinking water by adsorption onto alum-impregnated activated alumina, Sep. Purif. Technol., 50 (2006) 310–317.
[21] M. Karthikeyan, K.P. Elango, Removal of fluoride from water using aluminium containing compounds, J. Environ. Sci., 21 (2009) 1513–1518.
[22] I. Mobasherpour, E. Salahi, M. Pazouki, Comparative of the removal of Pb2+, Cd2+ and Ni2+ by nano crystallite hydroxyapatite from aqueous solutions: adsorption isotherm study, Arabian J. Chem., 5 (2012) 439–446.
[23] L. Lv, P. Sun, Z. Gu, H. Du, X. Pang, X. Tao, R. Xu, L. Xu, Removal of chloride ion from aqueous solution by ZnAl-NO3 layered double hydroxides as anion-exchanger, J. Hazard. Mater., 161 (2009) 1444–1449.
[24] C. Li, J. Gao, J. Pan, Z. Zhang, Y. Yan, Synthesis, characterization, and adsorption performance of Pb(II)-imprinted polymer in nano-TiO2 matrix, J. Environ. Sci., 21 (2009) 1722–1729.
[25] S.S. Tripathy, A.M. Raichur, Enhanced adsorption capacity of activated alumina by impregnation with alum for removal of As(V) from water, Chem. Eng. J., 138 (2008) 179–186.
[26] W. Ma, F.-Q. Ya, M. Han, R. Wang, Characteristics of equilibrium, kinetics studies for adsorption of fluoride on magnetic-chitosan particle, J. Hazard. Mater., 143 (2007) 296–302.
[27] I. Langmuir, The adsorption of gases on plane surfaces of glass, mica and platinum, J. Am. Chem. Soc., 40 (1918) 1361–1403.
[28] Y.S. Ho, G. McKay, Pseudo-second order model for sorption processes, Process Biochem., 34 (1999) 451–465.
[29] Z. Aksu, Determination of the equilibrium, kinetic and thermodynamic parameters of the batch biosorption of nickel(II) ions onto Chlorella vulgaris, Process Biochem., 38 (2002) 89–99.
[30] S. Rengaraj, Y. Kim, C.K. Joo, J. Yi, Removal of copper from aqueous solution by aminated and protonated mesoporous aluminas: kinetics and equilibrium, J. Colloid Interface Sci., 273 (2004) 14–21.
[31] Z.A. Al-Anber, M.A.S. Al-Anber, Thermodynamics and kinetic studies of iron(III) adsorption by olive cake in a batch system, J. Mex. Chem. Soc., 52 (2008) 108–115.
[32] B.S. Krishna, N. Mahadevaiah, D.S.R. Murty, B.S.J. Prakash, Surfactant immobilized interlayer species bonded to montmorillonite as recyclable adsorbent for lead ions, J. Colloid Interface Sci., 271 (2004) 270–276.
[33] S.H. Chien, W.R. Clayton, Application of Elovich equation to the kinetics of phosphate release and sorption in Soils1, Soil. Sci. Soc. Am. J., 44 (1980) 265–268.
[34] M. Yurdakoç, Y. Seki, S. Karahan, K. Yurdakoç, Kinetic and thermodynamic studies of boron removal by Siral 5, Siral 40, and Siral 80, J. Colloid Interface Sci., 286 (2005) 440–446.